Barriers to Stereoinversion of *N*-Aryl-1,3,2-benzodithiazole 1-Oxides Studied by Dynamic Enantioselective Liquid Chromatography

Joakim Oxelbark and Stig Allenmark*

Department of Chemistry, Göteborg University, SE-41296 Göteborg, Sweden

Received September 16, 1998

Free energies of activation for the enantiomerization of a series of racemic *N*-aryl-1,3,2-benzodithiazole 1-oxides have been determined by dynamic high-performance liquid chromatography (DHPLC) on a chiral stationary phase. From a comparison of experimental and computer-simulated chromatograms, the barriers to stereoinversion at sulfur were found to be around 80 kJ/mol and relatively insensitive to effects from substituents in the *N*-aryl group. Throughout the series the (+)-forms (436 nm) were found to be of (*S*)-configuration.

Introduction

In our continuing investigation of the configurational stability and chiroptical properties of *N*-substituted 1,3,2-benzodithiazole 1-oxides, we have found that the *N*-benzyl-substituted compound (**1a**) exhibits a remarkably low barrier to stereoinversion at sulfur of about 95 kJ/mol.[1] Changes in the ring system were found to raise this barrier quite dramatically. The low stereointegrity was first observed by Klein et al.,[2] who synthesized compounds of this type for studies of their antifungal activity. Because sulfoxides have been shown to enantiomerize via several different pathways, we have been interested in determining the mechanism of this stereoinversion. Usually, sulfoxides enantiomerize by a pyramidal inversion mechanism, the barrier being about 160 kJ/mol.[3] 2,5-Di-*tert*-octylthiophene sulfoxide, however, the most stereolabile (although achiral) sulfoxide prepared, is known to undergo pyramidal inversion, with a barrier of only 60 kJ/mol.[4] This process has been suggested to be facilitated by aromatic stabilization of the pseudoplanar transition state. Aryl sulfinamides[5] and benzylic sulfoxides,[6] on the other hand, have been shown to enantiomerize by a radical homolysis mechanism, and allylic sulfenates[7] via a reversible sigmatropic rearrangement.

To gain further insight into this problem, a series of *N*-phenyl-substituted 1,3,2-benzodithiazole 1-oxides (**1b**−**d**), Chart 1, was synthesized. These compounds were thought to permit an extended charge delocalization in the transition state, or to stabilize a possible diradical, thus increasing the enantiomerization rate. The low barrier to stereoinversion of these compounds makes them suitable for studies by dynamic HPLC (DHPLC), a technique[8] similar to dynamic NMR (DNMR) although applicable within a different time scale. The shape of the chromatogram of the resolved racemate is dependent on the interconversion rate of the enantiomers. At a certain temperature the racemate will collapse into a single broadened peak due to the fast enantiomerization. This process is possible to computer simulate, and by comparison with experimental data, the rate constants of the interconversion process can be determined. DHPLC has been shown to produce results in good agreement with those obtained by independent techniques,[9] except for the rare case when the stationary phase shows catalytic activity.[10] The rapid enantiomerization of compounds **1b**−**e** makes isolation of the enantiomers very difficult, and DHPLC thus proved to be a simple and effective way to determine their barriers to inversion. In this work DNMR was excluded because of the high temperatures needed and the limited stability of the analytes.

Chart 1

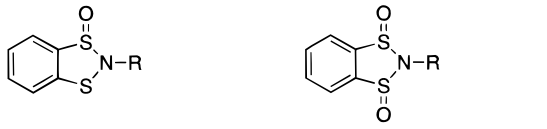

1a: R= benzyl
1b: R= 3,4,5-trimethoxyphenyl
1c: R= p-methoxyphenyl
1d: R= phenyl
1e: R= p-nitrophenyl

2a: R= benzyl
2b: R= 3,4,5-trimethoxyphenyl
2c: R= p-methoxyphenyl
2d: R= phenyl
2e: R= p-nitrophenyl

Results and Discussion

The barriers to stereoinversion of **1b**−**e** were determined to around 80 kJ/mol using DHPLC as shown in

(1) (a) Allenmark, S.; Oxelbark, J. *Enantiomer* **1996**, *1*, 13−22. (b) Allenmark, S.; Oxelbark, J. *Chirality* **1997**, *9*, 638−642.
(2) Klein, L. L.; Yeung, C. M.; Weissing, D. E.; Lartey, P. A.; Tanaka, K.; Plattner, J. J.; Mulford, D. J. *J. Med. Chem.* **1994**, *37*, 572−578.
(3) Rayner, D. R.; Gordon, A. J.; Mislow, K. *J. Am. Chem. Soc.* **1968**, *90*, 4854−4860.
(4) (a) Mock, W. L. *J. Am. Chem. Soc.* **1970**, *92*, 7610−7612. (b) Jenks, W. S.; Matsunaga, N.; Gordon, M. *J. Org. Chem.* **1996**, *61*, 1275−1283.
(5) Booms, R. E.; Cram, D. J. *J. Am. Chem. Soc.* **1972**, *94*, 5438−5446.
(6) Miller, E. G.; Rayner, D. R.; Thomas, H. T.; Mislow, K. *J. Am. Chem. Soc.* **1968**, *90*, 4861−4868.
(7) Bickart, P.; Carson, F. W.; Jacobus, J.; Miller, E. G.; Mislow, K. *J. Am. Chem. Soc.* **1968**, *90*, 4869−4876.
(8) (a) Bürkle, W.; Karfunkel, H.; Schurig, V. *J. Chromatogr.* **1984**, *288*, 1−14. (b) Jung, M.; Schurig, V. *J. Am. Chem. Soc.* **1992**, *114*, 529−534. (c) Veciana, J.; Crespo, M. I. *Angew. Chem., Int. Ed. Engl.* **1991**, *30*, 74−76. (d) Eiglsperger, A.; Kastner, F.; Mannschreck, A. *J. Mol. Struct.* **1985**, *126*, 421−432. (e) Mannschreck, A.; Andert, D.; Eiglsperger, A.; Gmahl, E.; Buchner, H. *Chromatographia* **1988**, *25*, 182−188. (f) Mannschreck, A.; Zinner, H.; Pustet, N. *Chimia* **1989**, *43*, 165−166.
(9) Gasparrini, F.; Lunazzi, L.; Misiti, D.; Villani, C. *Acc. Chem. Res.* **1995**, *28*, 163−170.
(10) Schurig, V.; Leyrer, U. *Tetrahedron: Asymmetry* **1990**, *1*, 865−868.

10.1021/jo981885o CCC: $18.00
Published on Web 02/13/1999

Table 1. Results of DHPLC Simulations

compd	$\Delta G^{\ddagger}_{app}$[a]/kJ mol^{-1}	temp/K[b]	runs[c]	range/K[d]
1b	81.0	274.4	10	11
1c	79.5	263.8	7	11
1d	81.1	256.5	3	4
1e	80.2	261.6	12	13

[a] Gibb's free energy calculated from the mean of k^{f}_{app} and k^{r}_{app}. [b] Mean temperature. [c] Number of simulated chromatograms. [d] Temperature range of the experimental chromatograms.

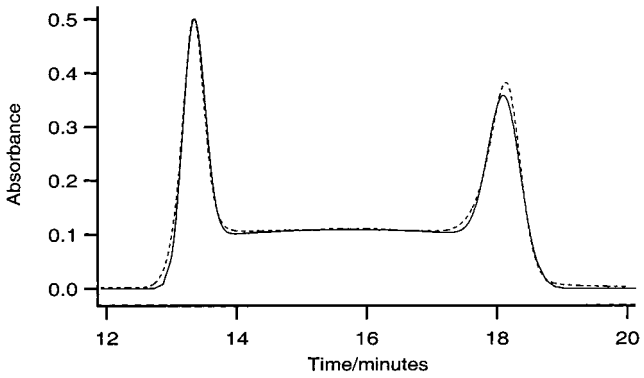

Figure 1. Experimental (···) and simulated (—) chromatograms of **1b** at −10 °C (Whelk-O1, 45% hexane and 1% methanol in dichloromethane, 0.5 mL/min). Parameters used: $t_M = 5.2$ min; $N = 3800$.

Scheme 1

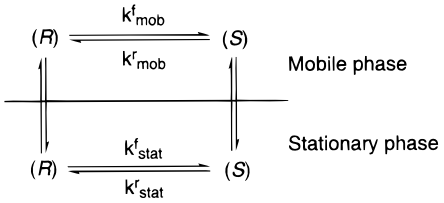

Table 1. The effect from the substituents on the phenyl ring on the enantiomerization rate is clearly within the error limit of the method. No trend can be distinguished in the $\Delta G^{\ddagger}_{app}$values given in Table 1. Extrapolation of the data to 260 K results in $\Delta G^{\ddagger}_{app(260)}$ values which should be comparable. This extrapolation does not change the relative order of the $\Delta G^{\ddagger}_{app}$values. The fit of the simulated chromatograms differs slightly among the different analytes but is generally quite satisfactory, as can be seen in Figure 1. Best fits were obtained for **1b**,**c** because they exhibit somewhat better peak shapes, i.e., tailing is less pronounced. A general observation is that the height of the second enantiomer peak in the simulated chromatograms is slightly lower than expected. This might be caused by the different number of theoretical plates found for the first and second enantiomers in the experimental chromatograms. Despite this slight mismatch, however, the experimental and simulated half-height widths seem to be almost identical. The equilibria[8a] involved in the overall enantiomerization process are shown in Scheme 1.

Chromatographic data for **1b**−**e** are given in Table 2. Polarimetric detection at 436 nm of the eluted enantiomers indicated a reversal of elution order in the series. The reversed elution order was confirmed by oxidizing enantiomerically enriched **1b**−**e**. It was found that oxidation of (+)-**1b**−**e** consistently yielded an excess of the last eluted enantiomer[11] of **2b**−**e**. Figure 2 shows the CD spectra in acetonitrile of these last eluted enantiomers and of (1*S*,3*S*)-**2a**,[1a] from which it is evident that they all have the same absolute configuration. This implies that compounds (+)-**1b**−**e** are all of the (*S*)-configuration. The previously reported[1a] (*R*)-configuration of (+)-**1a** refers to the optical rotation at 302 nm, which is opposite in sign to that obtained at 436 nm. In the present work all optical rotations were measured at 436 nm.

Table 2. Selected Chromatographic Data[a]

compd	k_1'	k_2'	α[b]	elution[c]	abs config[d]
1b	1.58	3.85	2.44	(−) (+)	(*R*)
1c	1.73	2.69	1.56	(−) (+)	(*R*)
1d	1.77	2.00	1.13	(+) (−)	(*S*)
1e	2.12	2.81	1.33	(+) (−)	(*S*)

[a] Column: (3*S*,4*R*) Whelk-O1 (200 × 4.6 mm). Flow rate: 1.0 mL/min. Mobile phase: 45% hexane in dichloromethane with 1% methanol added. Temperature: −18 °C. [b] $\alpha = k_2'/k_1'$. [c] Elution order determined at 436 nm. [d] Absolute configuration of the first eluted enantiomer.

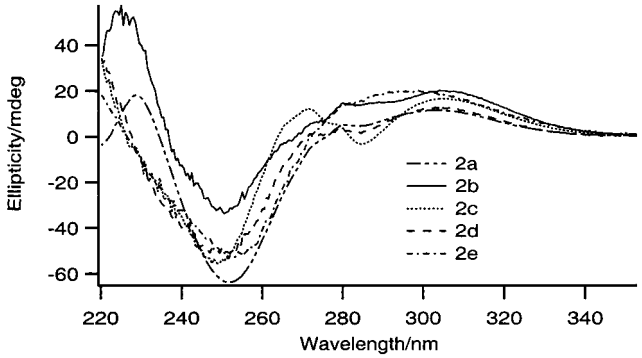

Figure 2. CD spectra of (1*S*,3*S*)-**2a** and the late-eluting enantiomers[11] of **2b**−**e** in acetonitrile (arbitrary concentrations used).

The bis(oxide)s obtained were composed of 80−95% of the meso diastereomers. Therefore, only small amounts of the enantiomers were prepared, except for **2d**, of which NMR and mass spectra of the respective diastereomers were recorded. Since the oxidation state of the ring system affects the position of the CD band at the longest wavelength quite significantly[1a] and the spectra of **2d** and the other isolated bis(oxide)s in the series (**2b,c,e**) show great similarities, there is no reason to doubt the identity of the latter, even though the amounts obtained were not sufficient for NMR analysis.

The low separation factor of **1d** is well explained by the reversal of the elution order. The chromatographic retention is influenced by the substituents in such a way that k'_R increases with the π-accepting ability of the aryl substituent, which is in accordance with what has been found[1b] for the different analogues of **1a**.

Experimental Section

Dynamic HPLC. Low-temperature HPLC[12] was carried out using a 5μ (3*S*,4*R*) Whelk-O1 sorbent[13] (Regis Technologies, Inc., Morton Grove, IL) in a 200 × 4.6 mm column immersed in a thermostated cooling bath. The column was connected to the injector by a steel capillary of ca. 1 m length, also immersed in the cooling bath. When the temperature was changed, the

(11) The column used was a 200 × 4.6 mm Kromasil CHI-DMB (EKA Chemicals Co., Bohus, Sweden). The mobile phase was composed of 15% ethyl acetate in cyclohexane, except for **2e**, for which neat tBME was used. Ethyl acetate was added to the solution injected, to increase the solubility.

system was left to equilibrate thermally for 20 min prior to chromatography. The mobile phase was composed of 45% *n*-hexane and 1% methanol in dichloromethane. UV detection was carried out at 240 nm.

Simulation of Chromatograms. Simulations of the experimental chromatograms were performed with a slightly modified[14] version of the SIMUL[15] program, which is based on the discontinuous plate model.[16] Plate number, retention times, and the void time of the column are determined experimentally. These figures together with rate constants for the reaction in the mobile and stationary phases, k_{mob} and k_{stat}, are used as input parameters. Rate constants are then changed until the simulated and experimental chromatograms show the best possible correspondence.

Determination of the plate number for the simulation turned out to be the crucial step in determining the reaction barrier. A change of ±500 plates causes only minor differences in peak width but is associated with a change in plateau height corresponding to a change in rate of up to ±10%. This should be compared with the error in rate arising from the uncertainty in fitting the height of the plateau, which is less than ±5%.

Use of the correct experimental plate number, i.e., eq 1, would produce too narrow peaks. This is due to the fact that

$$N = 5.54(t_R^2/w_h^2) \quad (1)$$

$$N = 5.54(t_R(t_R - t_M)/w_h^2) \quad (2)$$

the discontinuous plate model does not take analyte diffusion into account. Therefore, as suggested in the program user's manual,[15] the plate number used for the simulation was determined according to eq 2, where t_R is the retention time of the analyte, t_M is the void time, and w_h is the half-height peak width.

Still, this determination is to some extent subjective, since the tailing and fronting experimental chromatograms are different from the Gaussian-shaped simulated ones, and what is considered a best fit is somewhat arbitrary.

The strategy was to determine the plate number of a few chromatograms with a plateau of about 10−40% of the peak height and to calculate a mean. This plate number was then used for the simulation of chromatograms with the same analyte and flow rate but at different temperatures. To permit a precise determination of the rate constants, the plateau must exceed 10% of the peak height. In principle, it would also be possible to determine the activation parameters of the reaction. In this particular case, however, the temperature range spanning the coalescence of the peaks is too narrow.

Rate constants in the stationary phase were arbitrarily set to $^1/_{10}$ of the rate constants in the mobile phase. The shape of the simulated chromatogram is determined by the apparent rate constants of the respective directions (k^f_{app} and k^r_{app}). k^f_{app} and k^r_{app} are nonequivalent due to the presence of the chiral selector and can be expressed as the k_{mob} and k_{stat} mean values weighted by the residence time in each phase.[8c] Because there is an infinite number of pairs of k_{stat} and k_{mob} yielding the same k_{app}, they can either be set equal or to a fixed ratio, unless k_{mob} is known from independent experiments. If, however, k_{mob} is found by an independent technique, k_{stat} can be obtained from the k_{app} values determined. To set k_{stat} lower than k_{mob} is justified by the fact that the barrier to enantiomerization in the stationary phase has been determined to be up to 5 kJ/mol higher than in the mobile phase.[14b] This study was performed using the Whelk-O1 phase and atropisomeric naphthamides as analytes. The result can be rationalized by the assumption that in the analyte/selector complex the transition state cannot be reached unless a hydrogen bond is partially broken.

Assignment of Absolute Configuration. The enantiomers of the monoxides **1b**−**d** were collected using enantioselective HPLC at −20 °C and immediately poured into a cooled (−20 °C) and dried solution of 1 equiv mCPBA in dichloromethane. After 20 min at this temperature the reaction mixture was worked up as fast as possible to prevent hydrolysis. Drying and solvent evaporation gave the bis(oxide)s **2b**−**e**. Each of these were analyzed by enantioselective chromatography[11] with respect to the location of the predominating enantiomer of the trans isomer. The enantiomer present in excess was isolated and its CD spectrum recorded. The CD spectra of these enantiomers of **2b**−**e** were then compared with the spectrum of (1S,3S)-**2a** in acetonitrile. Compound **2d** was prepared on a larger scale, allowing for NMR and MS analysis of the meso and racemic form.

2-Aryl-1,3,2-benzodithiazoles: General Procedure. A solution of the appropriate aniline (8 mmol) and triethylamine (16 mmol, 1.62 g) in 20 mL of dry THF was added dropwise to a cooled (−70 °C) and stirred solution of benzene-1,2-disulfenyl chloride (8 mmol, 1.69 g) in 120 mL of dry THF under nitrogen. The solution was left to thaw slowly (a few hours) and then kept overnight at room temperature. The solution was filtered and evaporated under reduced pressure to yield a black, tarry oil. Filtration through silica as a chloroform solution was followed by flash chromatography with 30% chloroform in hexane as the eluent.

2-(3,4,5-Trimethoxyphenyl)-1,3,2-benzodithiazole: ^{1}H NMR (400 MHz, $CDCl_3$) δ 3.75 (s, 3H), 3.80 (s, 6H), 6.62 (s, 2H), 7.15−7.20 (m, 2H), 7.36−7.41 (m, 2H); ^{13}C NMR (101 MHz, $CDCl_3$, ^{1}H-decoupled) δ 56.02, 60.82, 97.83, 120.50, 126.49, 135.13, 138.04, 150.39, 152.69.

2-(4-Methoxyphenyl)-1,3,2-benzodithiazole: ^{1}H NMR (400 MHz, $CDCl_3$) δ 3.72 (s, 3H), 6.70−6.74 (m, 2H), 7.14−7.19 (m, 2H), 7.22−7.27 (m, 2H), 7.35−7.40 (m, 2H); ^{13}C NMR (101 MHz, $CDCl_3$, ^{1}H-decoupled) δ 55.43, 113.65, 120.15, 121.92, 126.37, 137.96, 148.16, 157.03.

2-Phenyl-1,3,2-benzodithiazole: ^{1}H NMR (400 MHz, $CDCl_3$) δ 6.94−7.00 (m, 1H), 7.03−7.08 (m, 2H), 7.13−7.19 (m, 2H), 7.26−7.30 (m, 2H), 7.33−7.37 (m, 2H); ^{13}C NMR (101 MHz, $CDCl_3$, ^{1}H-decoupled) δ 120.16, 120.34, 124.69, 126.50, 128.68, 138.19, 154.18.

2-(4-Nitrophenyl)-1,3,2-benzodithiazole: ^{1}H NMR (400 MHz, $CDCl_3$) δ 7.18−7.22 (m, 2H), 7.40−7.44 (m, 2H), 7.52−7.56 (m, 2H), 8.08−8.13 (m, 2H); ^{13}C NMR (101 MHz, $CDCl_3$, ^{1}H-decoupled) δ 119.21, 120.46, 124.35, 126.82, 131.50, 143.65, 159.12.

2-Aryl-1,3,2-benzodithiazole *S*-Oxides. The oxidations were carried out as described previously.[1b]

2-(3,4,5-Trimethoxyphenyl)-1,3,2-benzodithiazole 1-oxide (1b): ^{1}H NMR (400 MHz, $CDCl_3$) δ 3.85 (s, 3H) 3.87 (s, 6H), 6.74 (s, 2H), 7.36−7.43 (m, 1H), 7.53−7.57 (m, 2H), 7.86−7.90 (m, 1H); ^{13}C NMR (101 MHz, $CDCl_3$, ^{1}H-decoupled) δ 56.23, 60.90, 101.84, 119.39, 125.73, 126.15, 131.43, 136.49, 136.89, 141.50, 141.91, 153.58; MS (FAB) *m/e* 337 (M), 338 (M + 1).

2-(4-Methoxyphenyl)-1,3,2-benzodithiazole 1-oxide (1c): ^{1}H NMR (400 MHz, $CDCl_3$) δ 3.80 (s, 3H) 6.86−6.91 (m, 2H), 7.32−7.38 (m, 1H), 7.39−7.44 (m, 2H), 7.49−7.53 (m, 2H), 7.83−7.87 (m, 1H); ^{13}C NMR (101 MHz, $CDCl_3$, ^{1}H-decoupled) δ 55.51, 114.56, 119.27, 125.65, 126.00, 126.81, 131.24, 133.25, 142.13, 142.21, 158.76; MS (FAB) *m/e* 277 (M), 278 (M + 1).

2-Phenyl-1,3,2-benzodithiazole 1-oxide (1d): ^{1}H NMR (400 MHz, $CDCl_3$) δ 7.06−7.12 (m, 1H), 7.20−7.28 (m, 3H), 7.32−7.44 (m, 4H), 7.71−7.75 (m, 1H); ^{13}C NMR (101 MHz, $CDCl_3$, ^{1}H-decoupled) δ 119.62, 123.12, 125.89, 126.28, 126.38, 129.76, 131.62, 141.17, 141.55, 141.97; MS (FAB) *m/e* 247 (M), 248 (M + 1).

(12) Temperatures down to −80 °C have been used successfully. See: (a) Wolf, C.; Pirkle, W. H.; Welch, C. J.; Hochmut, D. H.; König, W. A.; Chee, G.-L.; Charlton, J. L. *J. Org. Chem*. **1997**, *62*, 5208−5210. (b) Villani, C.; Pirkle, W. H. *Tetrahedron: Asymmetry* **1995**, *6*, 27−30.

(13) (a) Formerly wrongly designated as (*R,R*). (b) Pirkle, W. H.; Brice, L. J.; Widlanski, T. S.; Roestamadji, J. *Tetrahedron: Asymmetry* **1996**, *7*, 2173-2176.

(14) (a) Only user interface modifications. (b) Gasparrini, F.; Misiti, D.; Pierini, M.; Villani, C. *Tetrahedron: Asymmetry* **1997**, *8*, 2069−2073.

(15) (a) QCPE Program No. 620. (b) Jung, M. *QCPE Bull*. **1992**, *12*, 52.

(16) See ref 8b and references therein.

2-(4-Nitrophenyl)-1,3,2-benzodithiazole 1-oxide (1e): ^{1}H NMR (400 MHz, $CDCl_3$) δ 7.42−7.48 (m, 1H), 7.54−7.66 (m, 4H), 7.92−7.96 (m, 1H), 8.26−8.31 (m, 2H); ^{13}C NMR (101 MHz, $CDCl_3$, ^{1}H-decoupled) δ 119.71, 119.89, 125.61, 126.13, 126.74, 132.32, 140.06, 140.86, 143.94, 147.17; MS (FAB) *m*/*e* 292 (M), 293 (M + 1).

***trans*-2-Phenyl-1,3,2-benzodithiazole 1,3-dioxide (*trans*-2d)**: ^{1}H NMR (400 MHz, $CDCl_3$) δ 7.45−7.53 (m, 3H) 7.61−7.67 (m, 2H), 7.82−7.87 (m, 2H), 7.96−8.01 (m, 2H); ^{13}C NMR (101 MHz, $CDCl_3$, ^{1}H-decoupled) δ 126.52, 129.38, 129.44, 129.94, 133.74, 135.13, 146.01.

***cis*-2-Phenyl-1,3,2-benzodithiazole 1,3-dioxide (*cis*-2d)**: ^{1}H NMR (400 MHz, $CDCl_3$) δ 7.43−7.53 (m, 3H) 7.55−7.67 (m, 2H), 7.82−7.87 (m, 2H), 8.00−8.06 (m, 2H); ^{13}C NMR (101 MHz, $CDCl_3$, ^{1}H-decoupled) δ 126.66, 128, 23, 129.06, 130.01, 133.24, 136.55, 146.10.

Acknowledgment. We thank Prof. F. Gasparrini and Prof. D. Misiti for placing their simulation program and computer facilities at our disposal. Special thanks are due to Dr. C. Villani for the kind help during the stay of J.O. in Rome. This work was supported by a grant (K-AA/KU 02508-321) from the Swedish Natural Science Research Council (NFR). A travel grant (to J.O.) within the Swedish−Italian exchange program of NFR is also gratefully acknowledged.

JO981885O